

Structural confinement-induced highly efficient deep-red emission and negative thermal quenching performances in Mn⁴⁺-activated Ca₇Mg₂Ga_{6-y}Al_yO₁₈:Mn⁴⁺ phosphors

Jinmei Huang,^a Pengfei Jiang, ^{*a}Zien Cheng,^a Rong Wang,^b Rihong Cong,^a Tao Yang^{*a}

^a College of Chemistry and Chemical Engineering, Chongqing University, Chongqing 401131, China

^b School of Metallurgy and Materials Engineering, Chongqing University of Science & Technology, Chongqing 401331, P. R. China

* Corresponding authors: pengfeijiang@cqu.edu.cn; taoyang@cqu.edu.cn.

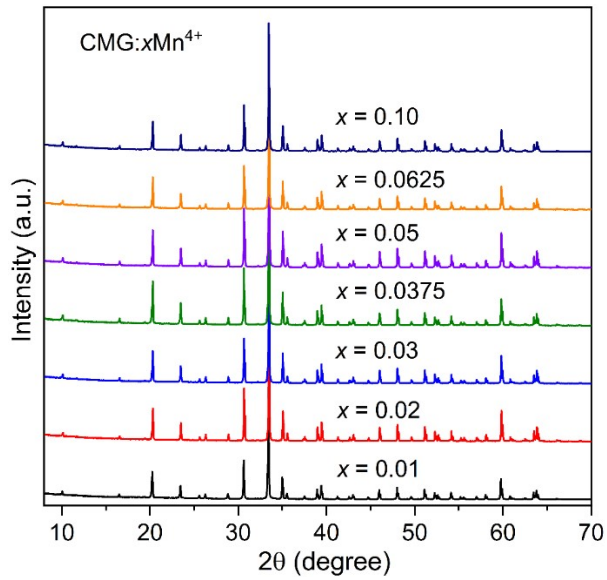


Fig. S1 XPRD patterns for CMGO: $x\text{Mn}^{4+}$ ($x = 0.01, 0.02, 0.03, 0.0375, 0.05, 0.0625$, and 0.10).

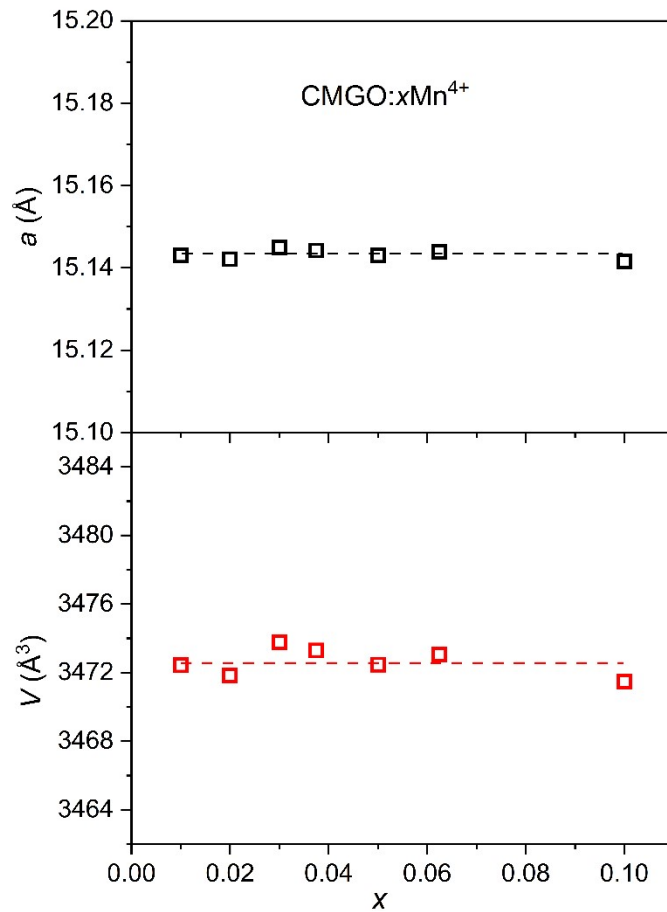


Fig. S2 Plots of lattice parameters along with Mn⁴⁺-content (x) in CMGO: $x\text{Mn}^{4+}$.

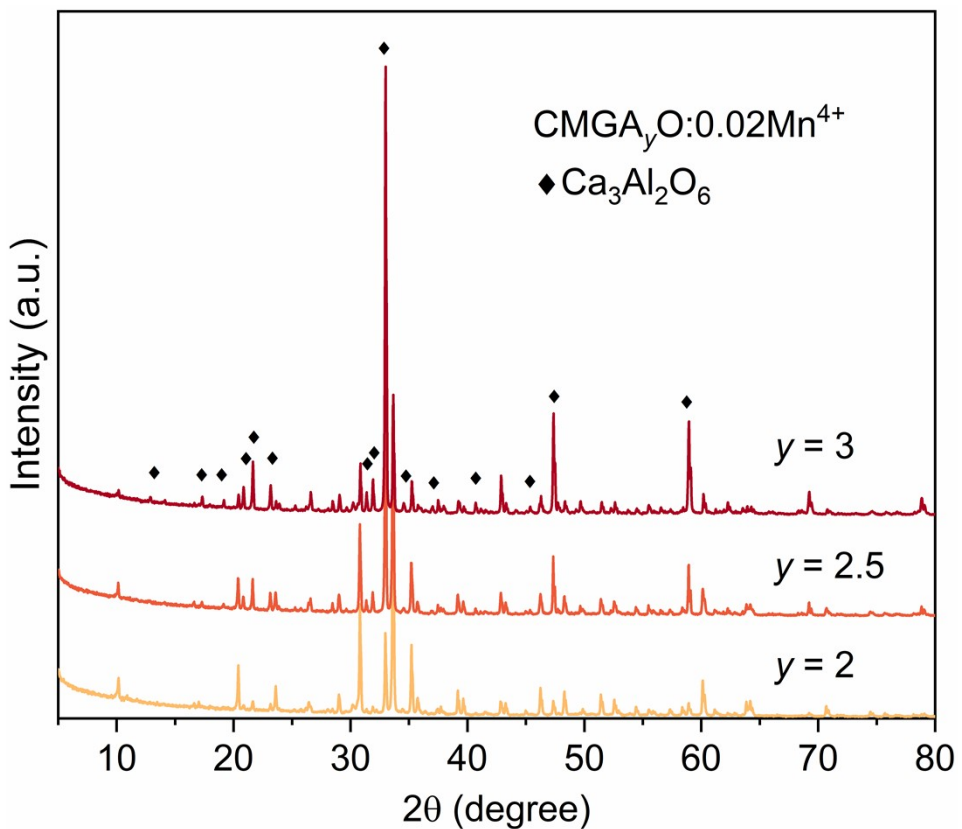


Fig. S3 PXRD patterns for $\text{CMGA}_y\text{O}:0.02\text{Mn}^{4+}$ with $y = 2, 2.5$, and 3 . The black diamonds represent the diffraction peaks corresponding to the impurity phase $\text{Ca}_3\text{Al}_2\text{O}_6$.

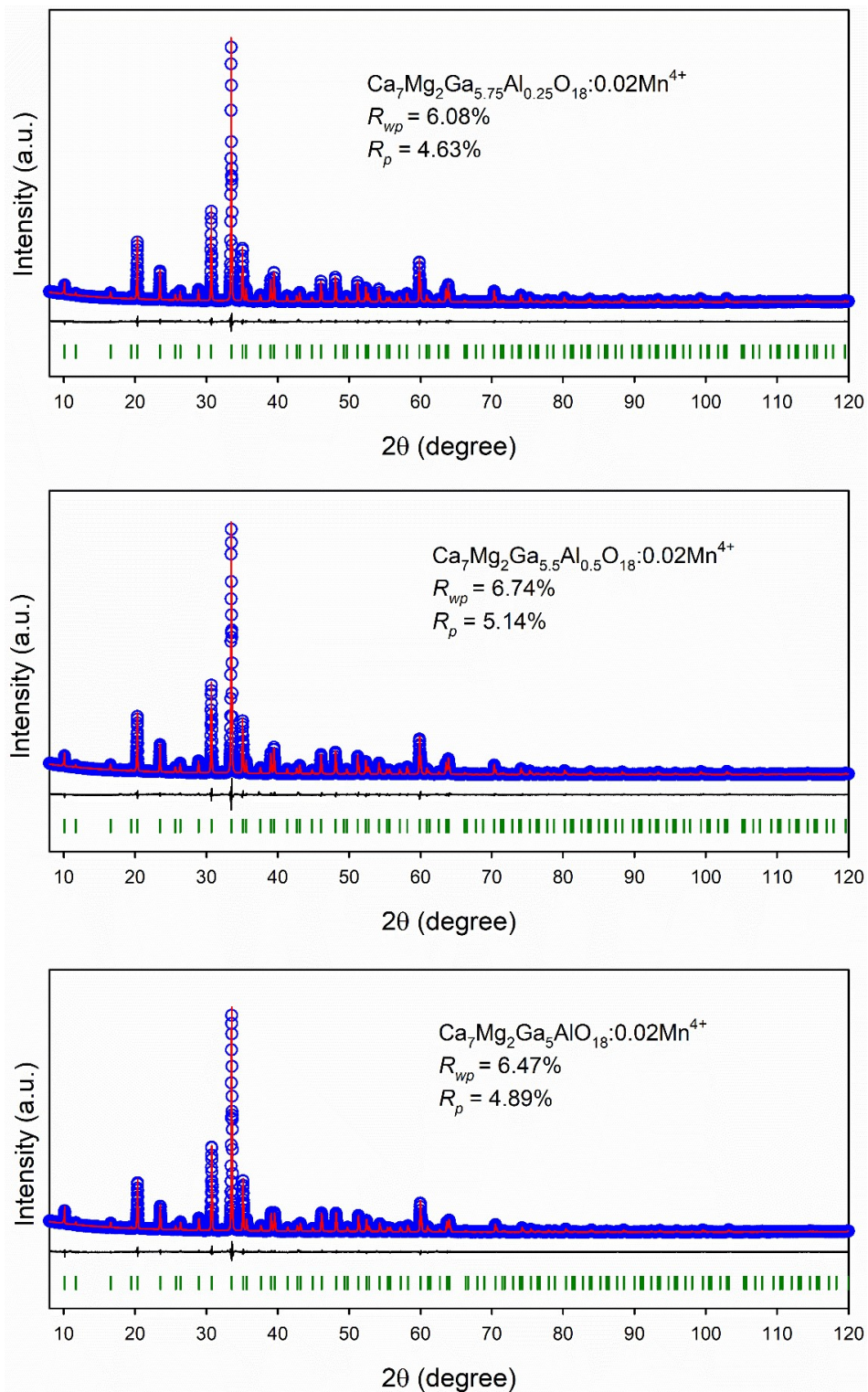


Fig. S4 Rietveld refinement plots of XPRD data for $\text{CMGA}_y\text{O}:\text{Mn}^{4+}$ ($y = 0.25, 0.5, \text{ and } 1$).

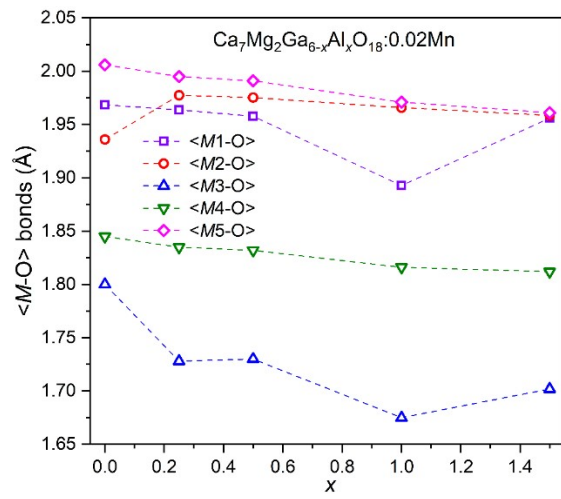


Fig. S5 Plots of the average metal-oxygen ($M\text{-O}$) bond lengths along with Al-content (y) in $\text{CMGA}_y\text{O:Mn}^{4+}$ ($y = 0, 0.25, 0.5, 1$, and 1.5).

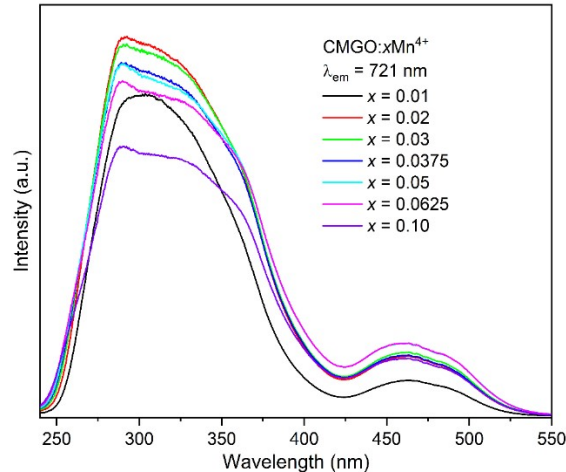


Fig. S6 The PLE spectra of $\text{CMGO}:x\text{Mn}^{4+}$ ($x = 0.01, 0.02, 0.03, 0.0375, 0.05, 0.0625$, and 0.10).

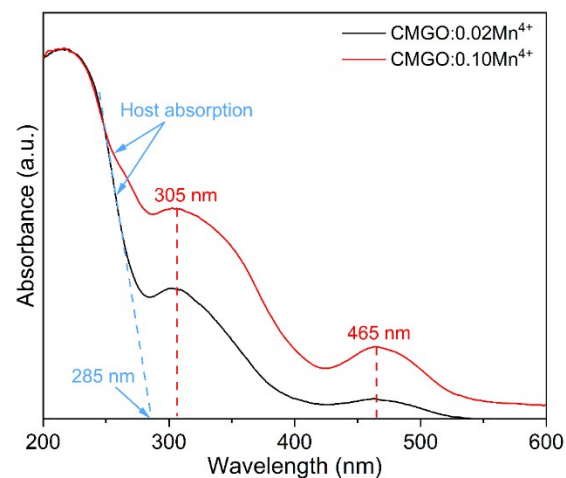


Fig. S7 The UV-visible light diffuse reflectance spectra for $\text{CMGO}:x\text{Mn}^{4+}$ ($x = 0.02$ and 0.10).

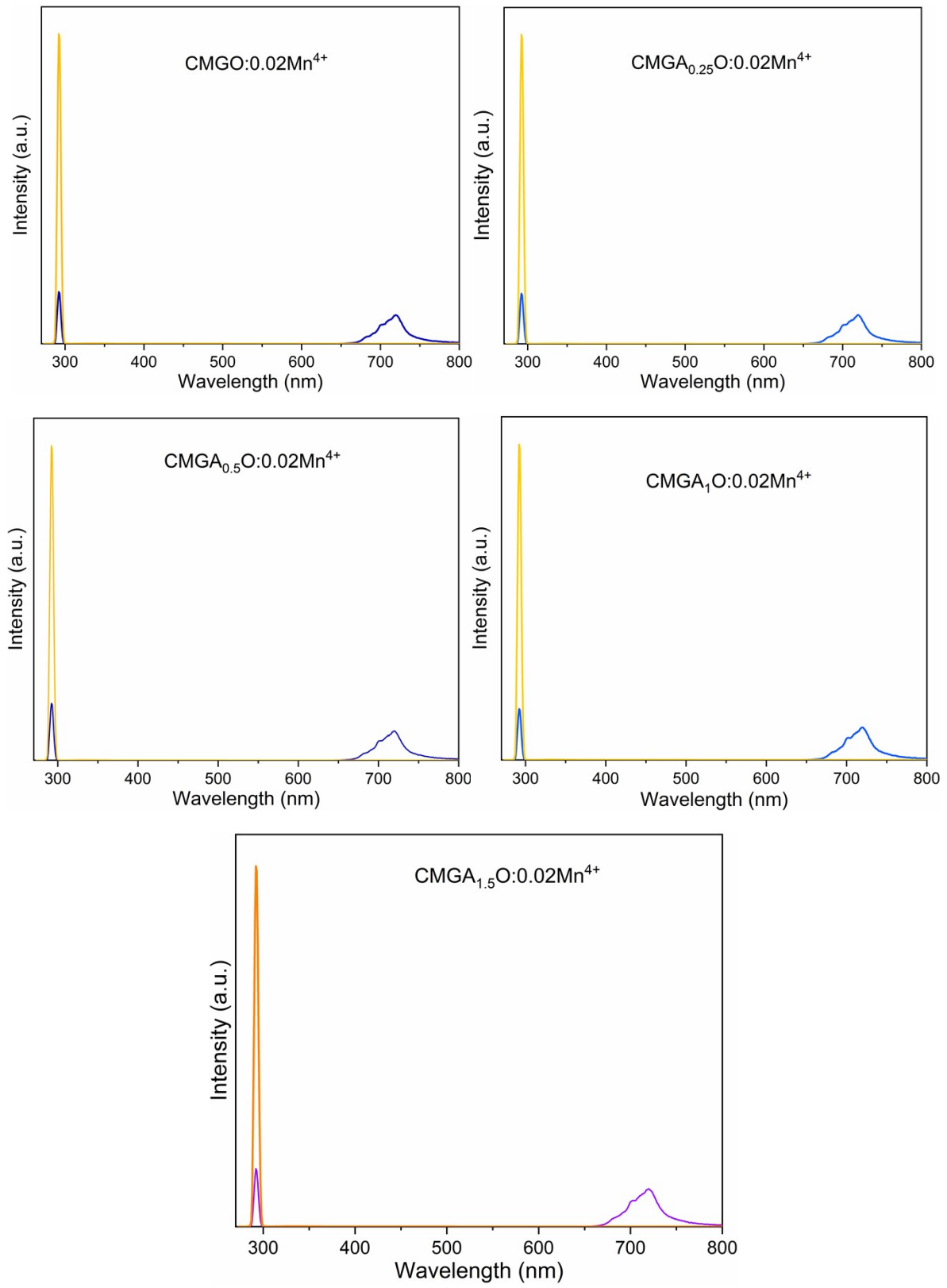


Fig. S8 The optical spectra of CMGA_yO:0.02Mn⁴⁺ phosphors recorded by the quantum efficiency system under the excitation wavelength of 293 nm. The yellow lines in the figures represent the reflectance of the BaSO₄ standard.

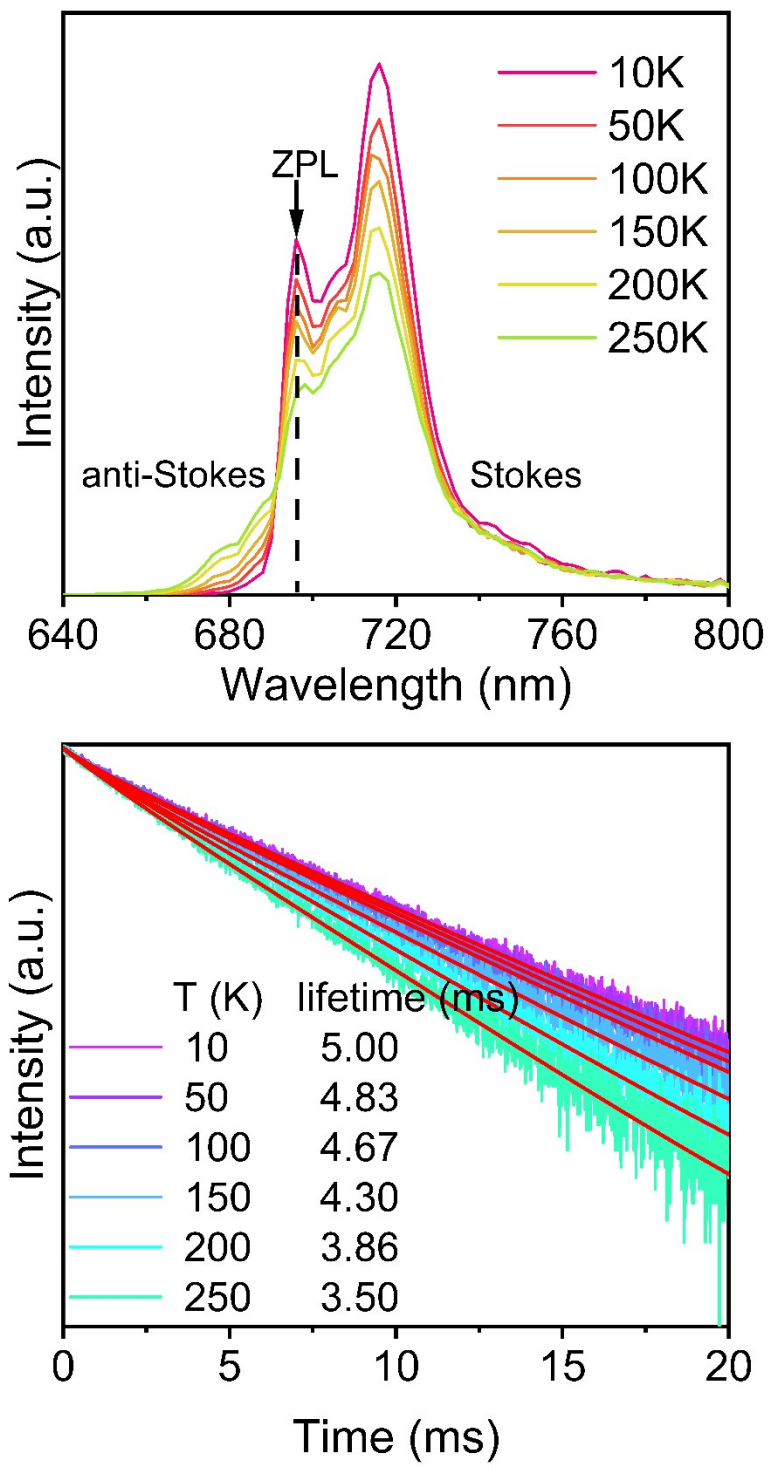


Fig. S9 Temperature-dependent PL spectra (up panel) and decay curves (down panel) of CMGO:0.02Mn⁴⁺ recorded at 10, 50, 100, 150, 200, and 250 K.

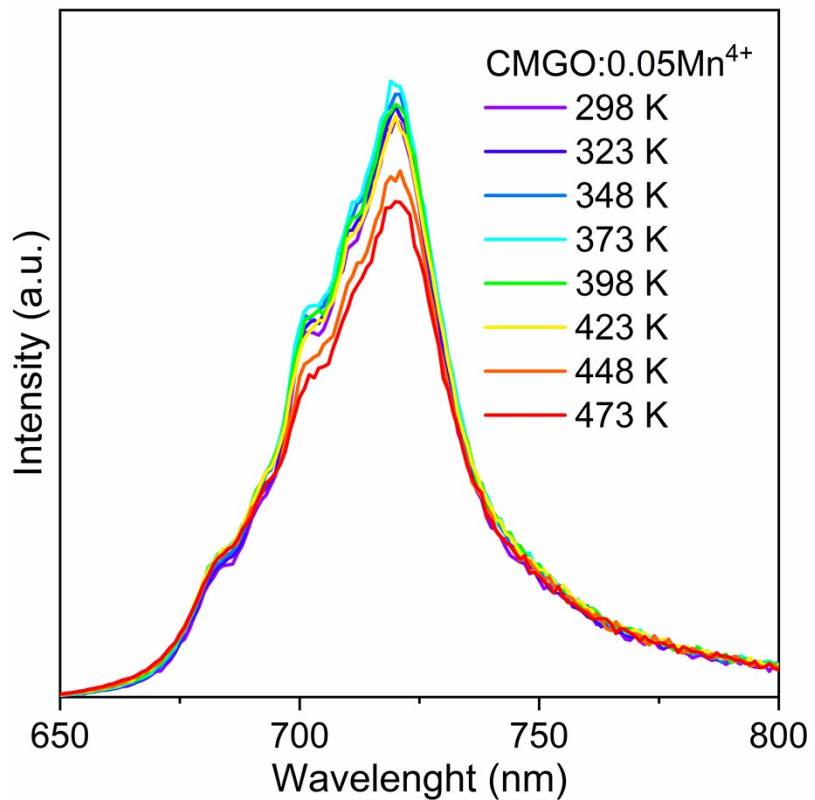


Fig. S10 Temperature-dependent PL spectra of CMGO:0.05Mn⁴⁺.

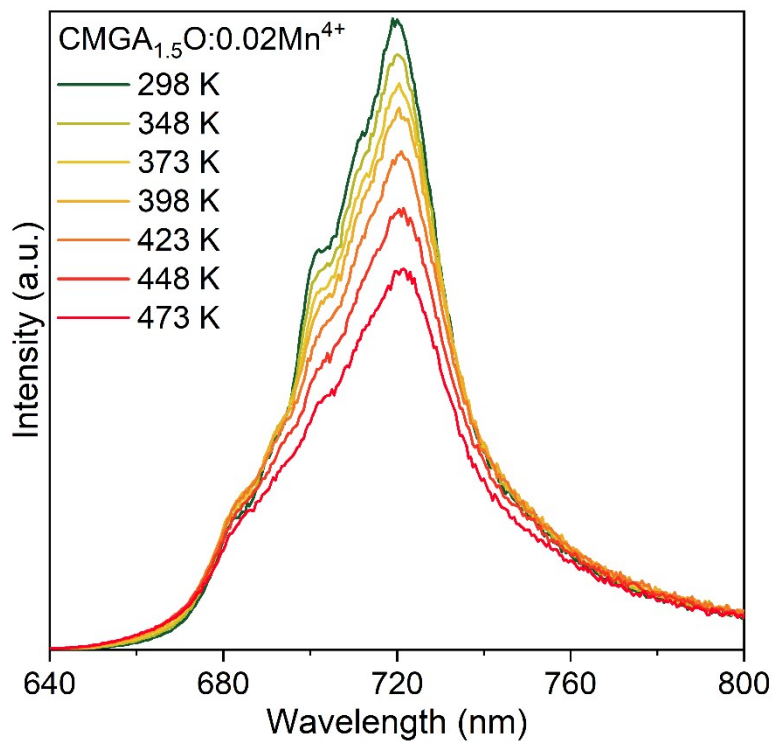


Fig. S11 Temperature-dependent PL spectra of CMGA_{1.5}O:0.02Mn⁴⁺.

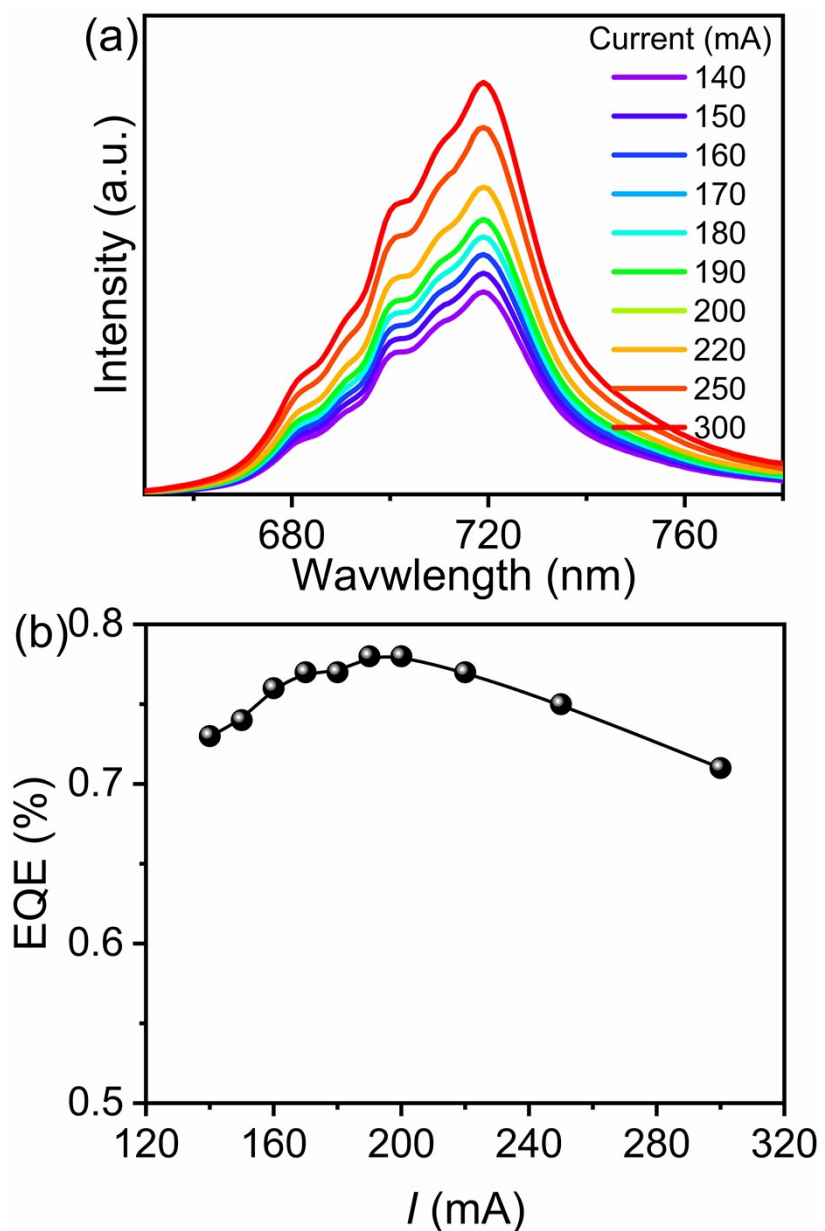


Fig. S12 Electroluminescence spectra (a) and measured EQE values (b) for the pc-LED fabricated by the combination of a 310 nm UV-chip and deep-red emitting phosphor CMGA_{1.5}O:Mn⁴⁺ under various driven currents.

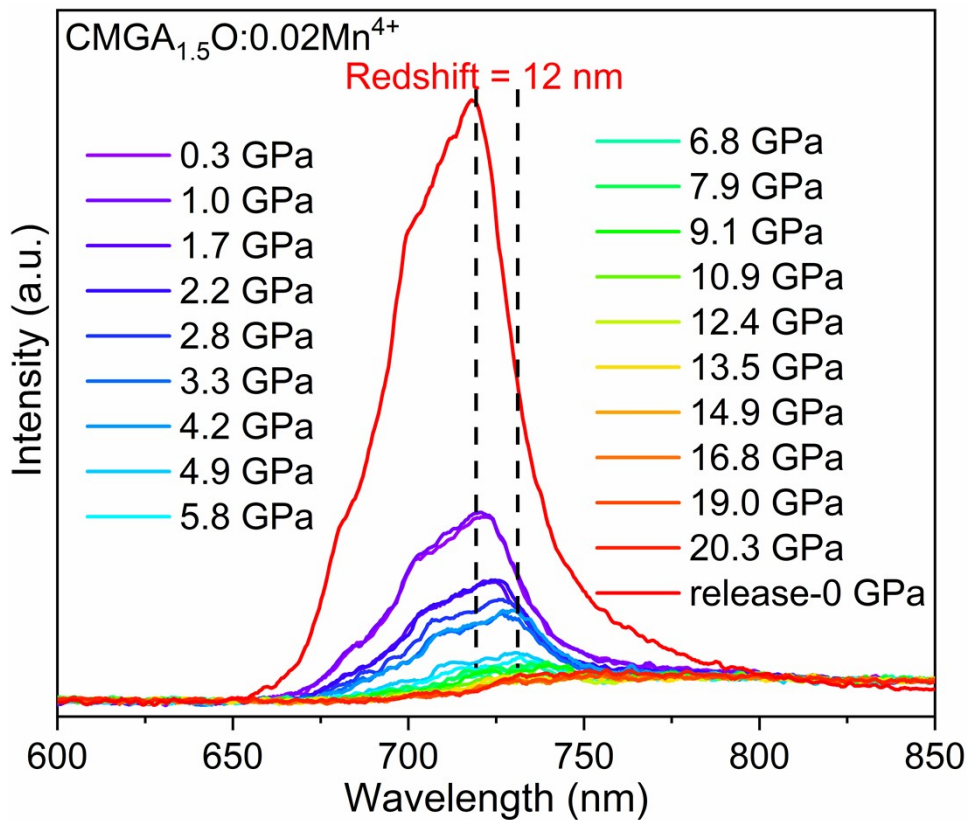


Fig. S13 The emission spectra ($\lambda_{\text{ex}} = 375$ nm) of CMGA_{1.5}O:0.02Mn⁴⁺ at different pressures.

Table S1 Fitted values for $h\nu_s$, a_1 , ΔE_1 , a_2 , and ΔE_2 .

Phosphors	$h\nu_s$ (meV)	a_1	ΔE_1 (meV)	a_2	ΔE_2 (eV)
CMGO:0.02Mn ⁴⁺	73.5	3.83	92.7	1.20×10^6	0.66
CMGO:0.05Mn ⁴⁺	73.8	1.59	72.3	1.20×10^6	0.63
CMA _{0.5} GO:Mn ⁴⁺	73.8	2.07	73.8	— [#]	— [#]
CMA _{1.5} GO:Mn ⁴⁺	73.6	3.82	88.1	1.14×10^6	0.59

[#] The “—” signs indicate these exponents are unnecessary in the mathematical fitting.